

Photonic crystal microcavities for chip-based cavity QED

Kartik Srinivasan*, Paul E. Barclay, and Oskar Painter

Department of Applied Physics, California Institute of Technology, Pasadena, CA 91125, USA

Received 19 July 2004, revised 21 July 2004, accepted 14 February 2005

Published online 24 March 2005

PACS 42.50.Pq, 42.60.Da, 42.70.Qs

The suitability of recently demonstrated high quality factor (Q), ultra-small mode volume (V_{eff}) graded square lattice photonic crystal microcavities for cavity QED experiments is discussed. In addition to the basic importance of the Q and V_{eff} of such cavities, other issues of both practical and fundamental relevance are considered. Included amongst these are the robustness of the cavity's performance to fabrication errors and the ability to efficiently source and collect light from the cavity through conventional fiber optics.

© 2005 WILEY-VCH Verlag GmbH & Co. KGaA, Weinheim

1 Introduction

Optical cavity quantum electrodynamics (cQED) has been successful in confirming some basic principles of quantum mechanics and in providing the underpinnings for future experiments in quantum information science and computing [1]. Within the latter disciplines, microchip-based cavities are appealing, in part due to the ability of planar fabrication to create, in parallel, multiple integrated devices, a prerequisite for some schemes in quantum networking and computation [2]. To that end, novel emitting devices employing semiconductor quantum dots within chip-based microdisk and micropillar cavities have already been demonstrated [3, 4]. In these works, the quality factor (Q) of the cavities were not high enough for coherent interactions (strong coupling) between single photons and single quantum dots to take place. The achievement of strong coupling within a semiconductor microcavity remains an important milestone in the development of chip-based cQED.¹

Planar photonic crystal (PC) microcavities (Fig. 1(a)) have a number of properties that are attractive for such experiments. Many of these properties are shared with other chip-based systems. As already mentioned, device arrays are easily fabricated on a chip, making the technology scalable. The cavities are formed in high refractive index semiconductors, including those in which narrow linewidth quantum dots can be grown. This integration of the quantum dot with the microcavity provides a level of simplification with respect to the cooling and trapping techniques required for atomic systems, particularly as control of the position of quantum dots continues to improve [5]. At the same time, because the field maxima in a PC microcavity can be located in either dielectric or air regions (not possible for microdisk or micropillar cavities), it can also be used to maximally interact with atoms or nanocrystals suspended in fluid. As atomic linewidths are still orders of magnitude less than those of the best quantum dots, experiments integrating semiconductor microcavities with cooled atoms are a potentially important sys-

* Corresponding author: e-mail: kartik@caltech.edu, Phone: (626) 395-6269, Fax: (626) 795-7258

¹ Note: Since submission of this manuscript, vacuum Rabi splitting in a semiconductor microcavity–quantum dot system has been demonstrated [J. Reithmaier et al., *Nature (London)* **432**, 197 (2004); T. Yoshie et al., *Nature (London)* **432**, 200 (2004); and E. Peter et al., Preprint quant-ph/0411076 (2004)].

tem for study. Furthermore, advances in magnetic microtraps for neutral atoms have made chip-level integration possible [6].

The basic criterion for strong coupling in cQED is for the coherent coupling rate between the photon and the atom (or quantum dot), labeled g , to exceed the decay rates of the cavity (κ) and the atom (γ). This coupling rate is proportional to the electric field strength within the cavity, and thus scales as $g \sim 1/\sqrt{V}$, where V is the volume to which the field is confined. In PC microcavities, V can approach the theoretical limit of $(\lambda/2n)^3$ (λ/n is the wavelength of light in the material). For coupling to a cesium atom, the corresponding predicted g values are tens of GHz, approximately three orders of magnitude larger than the current values seen in Fabry–Perot cavities [7]. The time scale for coherent interactions is thus very fast in PC cavities, and this will dictate the speed of any computation that involves energy transfer between the atom and photon. Furthermore, these g factors imply that cavity Q s of only $\sim 10^4$ are required to achieve $g > \kappa$ ($\kappa = \omega/2Q$). Such Q s, orders of magnitude less than that required for Fabry–Perot cavities, have long been predicted to be achievable, and recent experimental demonstrations of $Q > 10^4$ in InP-based [8] and Si-based [9, 10] PC cavities have confirmed these calculations. Due to the monolithic nature of semiconductor microcavities, these Q s are achieved without active cavity stabilization, an important experimental simplification. In the remainder of this article, we consider the properties of the graded lattice PC microcavities studied in Refs. [8, 10], and discuss their suitability for on-chip cQED.

2 Graded square lattice PC microcavities

The geometry of interest is shown in Fig. 1, and consists of a graded square lattice of air holes in a semiconductor membrane. The dielectric lattice provides in-plane modal confinement through distributed Bragg reflection (DBR), while the air-semiconductor index contrast in the vertical dimension confines light by total internal reflection. This cavity is predicted, through finite-difference time-domain (FDTD) simulations, to support a mode with $Q \sim 10^5$ and an effective modal volume $V_{\text{eff}} \sim (\lambda/n)^3$ (V_{eff} is defined relative to the peak electric field energy density in the structure, while V is defined relative to the peak field intensity. This is taken into account in subsequent calculations).

Details of device fabrication in InP-based and Si membranes have been presented elsewhere [8, 10]; the basic steps include electron beam lithography to define the lattice, transfer to an underlying dielectric mask through plasma dry etching (only for InP cavities), dry etching into the semiconductor layer, and wet chemical etching to create an undercut geometry. Fabricated devices in InP had a lattice constant $a \sim 325$ nm and those in Si (Fig. 1(b)) had $a \sim 400$ nm, to create cavity resonances in the 1300 nm and 1600 nm bands, respectively. Cavities in the InP-based material were probed through optical pumping of an embedded multi-quantum-well layer, with the measured emission linewidth (centered at 1.3 μm) at material transparency used to determine a cold-cavity $Q \sim 13,000$ [8]. Passive cavities in Si were probed directly using an external fiber taper waveguide (Fig. 1(c) and Section 4) that can source and out-couple the cavity modes; this novel measurement tool can directly probe both Q and V_{eff} , and a cavity with $Q \sim 40,000$ and a spatial localization consistent with $V_{\text{eff}} \sim 0.9(\lambda/n)^3$ has been demonstrated [10].

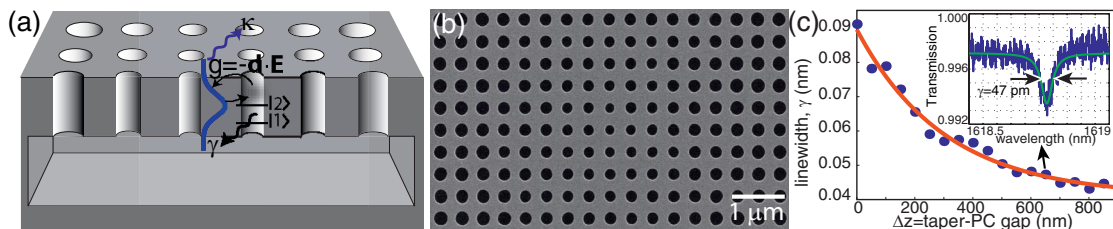


Fig. 1 (online colour at: www.pss-b.com) (a) Schematic of a PC microcavity whose mode is coupled to a two-level atom. (b) Scanning electron microscope (SEM) image of a fabricated Si microcavity. (c) Linewidth measurement of a Si microcavity through direct fiber taper probing. The inset shows the resonance in the taper’s transmission due to coupling to the cavity. Studying the variation of the resonance linewidth as a function of the taper-PC gap gives an estimate of the unloaded $Q \sim 40,000$.

For the latter device (operating at a wavelength $\lambda_0 \sim 1619$ nm), the corresponding maximal coupling rate to a Cs atom is predicted to be $g/(2\pi) \sim 16.1$ GHz [10], exceeding the cavity decay rate $\kappa/(2\pi) \sim 4.4$ GHz and atomic decay rate $\gamma/(2\pi) \sim 2.6$ MHz, and is thus in the strong coupling regime. More detailed calculations using the quantum master equation confirm that strong coupling effects between a single atom and a single photon should be observable [6]. Similarly, a simple estimate of g for coupling to a quantum dot with a lifetime $\tau \sim 1$ ns indicates that strong coupling is possible in this purely solid state system.

3 Robust cavity design

From a fundamental standpoint, demonstration of a cavity with a high enough Q and small enough V_{eff} so that $g > \kappa$ determines whether the cavity is suitable for strongly-coupled cQED experiments. In practice, there are other considerations taken into account when evaluating the feasibility of an experiment. For example, as mentioned above, an advantage in using a chip-based microcavity is that active stabilization is not required to maintain the requisite Q . This is somewhat mitigated if consistently obtaining cavities that exhibit such Q s is difficult. Processing of PC devices is challenging, and replicating a design in a fabricated device can be difficult. This in part explains why PC microcavities with $Q > 10^4$ have only recently been demonstrated even though designs predicting such Q s were proposed years earlier.

Our approach to this challenge [11] was to develop designs robust to fabrication-induced errors, so that Q s remain $> 10^4$. This philosophy was a major reason why the graded lattice geometry was adopted. While some designs rely on precise positioning or size of a small number of lattice holes to support a high- Q mode [9], the graded lattice design relies on more general aspects of the cavity. In particular, the symmetry of the cavity (and its resulting mode) is used to reduce vertical radiation losses [11], and mode-matching between the central part of the cavity (where the mode sits) and its exterior is achieved adiabatically through the grade in hole radius. Both of these techniques for reducing loss are relatively insensitive to changes in the size and shape of individual holes, making them tolerant to fabrication errors.

The robustness of these cavities was confirmed in both FDTD simulations and experimental measurements of fabricated Si cavities [11]. Cavities with significantly different average hole radii (varied by $> 30\%$) and steepness of grade were simulated and tested, and the Q s remained above 10^4 . In particular, in experiments, the frequency of the cavity mode varied by more than 10% of the nominal value while the Q remained between 13,000–40,000. In addition, V_{eff} for all of these devices was calculated to be between $0.8 - 1.4(\lambda/n)^3$. This ability to create arrays of high- Q , small V_{eff} cavities will be practically important; if one of the cavities in an array is resonant with a quantum dot exciton transition, for example, it will also likely have the requisite Q and V_{eff} for strong coupling.

4 Input-output coupling to PC microcavities

Another matter of considerable importance is the ability to efficiently source and extract light from the cavity; in particular, for the low light intensities within the cavity in cQED experiments [6], maximizing the amount of out-coupled signal from the interaction is necessary. In a standard Fabry–Perot cavity, the solution is perhaps obvious; one of the etalon mirrors is made to have slightly lower reflectivity. This causes a degradation of the cavity Q , but this additional loss is ‘good’ in the sense that it can be collected to comprise the measurement signal. Similarly, in a micropillar cavity, the top DBR mirror can be tailored to allow light to leak vertically into the air, where it can be efficiently collected into an optical fiber [3]. However, in PC microcavities, the solution is not necessarily straightforward; their wavelength-scale modal patterns are typically not suited for direct mode-matching to the much larger standard free-space and fiber optics. One solution is to integrate the cavity with an on-chip photonic crystal waveguide (PCWG) [9], and then use various end-fire based approaches to couple into and out of the PCWG. Despite significant improvement in techniques for such end-fire coupling, losses of > 1 dB per coupling junction can still be expected in such systems [12].

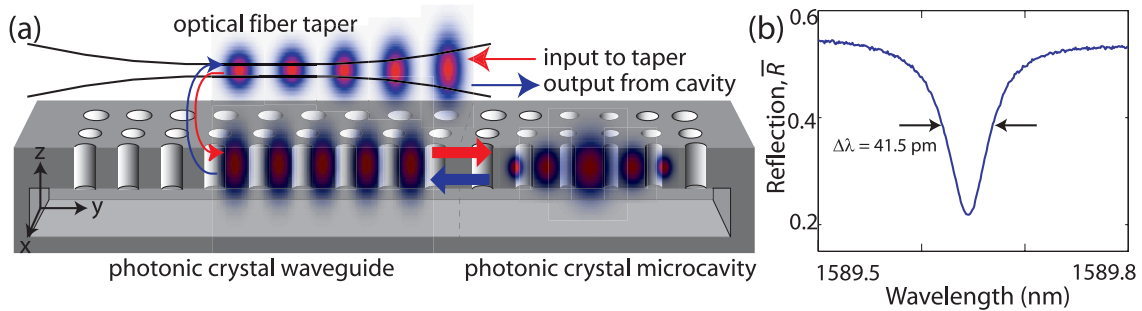


Fig. 2 (online colour at: www.pss-b.com) Fiber-coupled PC microcavity. (a) Input–output coupling: (i) the taper adiabatically converts light injected into its input to a micron-scale field, (ii) light is contradirectionally coupled to a phase-matched PCWG with high (>95%) efficiency, (iii) light tunnels from the end of the PCWG into a mode-matched PC cavity, (iv) coupling from the cavity back to the fiber follows the reverse process, so that the output from the cavity is detected in the reflected signal at the fiber input. (b) Measurement of such a device; the linewidth of the dip in the reflected signal corresponds to a loaded $Q \sim 38,000$. From the value of the off-resonance transmission, an unloaded $Q \sim 47,000$ is estimated.

Our approach to coupling into PC chips uses optical fiber tapers. The taper adiabatically converts light, with very low loss ($\leq 10\%$), from the mode of a standard single mode fiber to that of a 1–2 μm air-clad cylindrical glass waveguide. At these diameters, the field of the cylindrical waveguide extends into the surrounding air, and can interact with a PC chip when brought close to it. We have used fiber tapers to directly probe the spectral and spatial properties (Q and V_{eff}) of the PC microcavities discussed in Section 2; this direct coupling from the fiber taper waveguide to the PC cavity yields maximum coupling depths of a few percent. However, when the coupling levels are strongest, the taper also significantly loads the cavity, introducing both ‘good’ loss (light coupled back into the taper from the cavity) and ‘bad’ loss (scattered light or light coupled into undesirable taper modes). For cQED applications, the goal is to obtain a requisite signal level without degrading the Q so far that the cavity is no longer in the strong coupling regime. The ability to do this is somewhat compromised by the amount of ‘bad’ loss present in this direct probing method; nevertheless, its simplicity makes it a candidate for use in future experiments.

To minimize the amount of ‘bad’ loss when coupling to the cavities, a new technique that makes use of an intermediate PCWG has been used [13]. In this approach (Fig. 2(a)), light is first efficiently (> 95%) transferred to the PC chip by phase-matched evanescent coupling between an optical fiber taper and a PCWG [14]. This coupling is so efficient because the PCWG has been designed to phase-match to the mode of the optical fiber taper (not the case in direct coupling between the fiber and cavity), and has a significant enough spatial overlap with it for near-complete power transfer over tens of microns. The PCWG is terminated by the PC cavity; the two devices have been designed to be mode-matched so that coupling between them is also very efficient. Thus, light propagates through the PCWG, and when it reaches the PC cavity termination, some amount of the light that is resonant with the cavity mode tunnels into it (the amount of tunneling can be adjusted by tailoring the PCWG-PC cavity junction). This light can then interact with material in the cavity (an atom or quantum dot, for example), and then tunnel back into the PCWG, where it will be transferred back into the reflected signal of the optical fiber for measurement. Experimental measurements (Fig. 2(b)) of fabricated Si devices have yielded an unoptimized fiber-to-cavity coupling efficiency of 44% for a cavity with a loaded (unloaded) Q of 38,000 (47,000).

5 Conclusions

Photonic crystal microcavities with sufficiently high Q s and small V_{eff} s for strong coupling experiments have been demonstrated. In addition, these cavities are robust to errors during the fabrication process and have been integrated with fiber optics for efficient sourcing and collection. Current efforts are focused on integration with cold atoms and semiconductor quantum dots for chip-based cQED.

Acknowledgement K. S. thanks the Hertz Foundation for its graduate fellowship support.

References

- [1] H. J. Kimble, Phys. Scr. T **76**, 127 (1998).
- [2] J. I. Cirac, P. Zoller, H. J. Kimble, and H. Mabuchi, Phys. Rev. Lett. **78**, 3221 (1997).
- [3] M. Pelton et al., Phys. Rev. Lett. **89**, 233602 (2002).
- [4] P. Michler et al., Science **290**, 2282 (2000).
- [5] K. Hennessy et al., Proc. SPIE (2004).
- [6] B. Lev et al., Nanotechnology **15**, S556 (2004).
- [7] J. McKeever et al., Nature (London) **425**, 268 (2003).
- [8] K. Srinivasan et al., Appl. Phys. Lett. **83**, 1915 (2003).
- [9] Y. Akahane, T. Asano, B.-S. Song, and S. Noda, Nature (London) **425**, 944 (2003).
- [10] K. Srinivasan, P. E. Barclay, M. Borselli, and O. Painter, Phys. Rev. B **70**, 081306(R) (2004).
- [11] K. Srinivasan, P. E. Barclay, and O. Painter, Opt. Express **12**, 1458 (2004).
- [12] M. Notomi, A. Shinya, S. Mitsugi, and H.-Y. Ryu, Opt. Express. **12**, 1551 (2004).
- [13] P. E. Barclay, K. Srinivasan, and O. Painter, Opt. Express **13**(3), 801 (2005).
- [14] P. E. Barclay, K. Srinivasan, M. Borselli, and O. Painter, Opt. Lett. **29**, 697 (2004).